
Princeton Plasma Physics Laboratory

PPPL-

PPPL-



Prepared for the U.S. Department of Energy under Contract DE-AC02-09CH11466.

Princeton Plasma Physics Laboratory

Report Disclaimers

Full Legal Disclaimer

This report was prepared as an account of work sponsored by an agency of the United States Government. Neither the United States Government nor any agency thereof, nor any of their employees, nor any of their contractors, subcontractors or their employees, makes any warranty, express or implied, or assumes any legal liability or responsibility for the accuracy, completeness, or any third party's use or the results of such use of any information, apparatus, product, or process disclosed, or represents that its use would not infringe privately owned rights. Reference herein to any specific commercial product, process, or service by trade name, trademark, manufacturer, or otherwise, does not necessarily constitute or imply its endorsement, recommendation, or favoring by the United States Government or any agency thereof or its contractors or subcontractors. The views and opinions of authors expressed herein do not necessarily state or reflect those of the United States Government or any agency thereof.

Trademark Disclaimer

Reference herein to any specific commercial product, process, or service by trade name, trademark, manufacturer, or otherwise, does not necessarily constitute or imply its endorsement, recommendation, or favoring by the United States Government or any agency thereof or its contractors or subcontractors.

PPPL Report Availability

Princeton Plasma Physics Laboratory:

<http://www.pppl.gov/techreports.cfm>

Office of Scientific and Technical Information (OSTI):

<http://www.osti.gov/bridge>

Related Links:

[U.S. Department of Energy](#)

[Office of Scientific and Technical Information](#)

[Fusion Links](#)

A Generalized Weight-Based Particle-In-Cell Simulation Scheme

W. W. Lee, T. G. Jenkins[†] and S. Ethier

Princeton Plasma Physics Laboratory, Princeton University, Princeton, NJ 08543

[†]*Present Address: Tech-X Corporation, 5621 Arapahoe Avenue, Boulder, CO 80303*

Abstract - A generalized weight-based particle simulation scheme suitable for simulating magnetized plasmas, where the zeroth-order inhomogeneity is important, is presented. The scheme is an extension of the perturbative simulation schemes developed earlier for particle-in-cell (PIC) simulations. The new scheme is designed to simulate both the perturbed distribution (δf) and the full distribution (full- F) within the same code. The development is based on the concept of multiscale expansion, which separates the scale lengths of the background inhomogeneity from those associated with the perturbed distributions. The potential advantage for such an arrangement is to minimize the particle noise by using δf in the linear stage of the simulation, while retaining the flexibility of a full- F capability in the fully nonlinear stage of the development when signals associated with plasma turbulence are at a much higher level than those from the intrinsic particle noise.

I. Introduction to Multiscale Gyrokinetics - Since the development of the weight-based perturbative simulation schemes [1, 2], gyrokinetic particle simulation has contributed greatly in understanding tokamak transport in realistic tokamak discharges. The discovery of the existence of ion temperature gradient (ITG) streamers and their eventual breakup by turbulence [3], and the relationship between global zonal flows and the nonlinear saturation of ITG turbulence [4] are the two early examples. The simulations on the ion momentum transport [5] and on the electron thermal transport [6], both carried out on the state-of-the-art massively parallel computers, are the most recent success stories. However, there has been a concern that these so-called perturbative (δf) scheme may not be able to handle the simulations in the fully developed turbulence in long time simulations, where particle weights associated with δf may become too large and/or the full- F scheme may be needed, for example, to account for sources and sinks. The present paper, based on our understanding, represents the first attempt to address this issue by using the multiscale expansion to smoothly connect δf and full- F simulation regimes.

The governing gyrokinetic equations in the small gyroradius limit of $k_{\perp}^2 \rho_i^2 \ll 1$ in the slab limit

are [7–9]:

$$\frac{dF}{dt} \equiv \frac{\partial F}{\partial t} + v_{\parallel} \frac{\partial F}{\partial x_{\parallel}} + \mathbf{v}_{E \times B} \cdot \frac{\partial F}{\partial \mathbf{x}} + \frac{q}{m} E_{\parallel} \frac{\partial F}{\partial v_{\parallel}} = 0 \quad (1)$$

and

$$(\rho_s/\lambda_D)^2 \nabla_{\perp}^2 \phi = -4\pi e(n_i - n_e), \quad (2)$$

where $\rho_i \equiv v_t/\Omega_i$ is the ion gyroradius, $\mathbf{v}_{E \times B} \equiv c\mathbf{E} \times \hat{\mathbf{b}}/B$ is the gyrocenter drift due to the perturbed electric field, $\mathbf{E} = \mathbf{E}_{\perp} + \mathbf{E}_{\parallel} = -\partial\phi/\partial\mathbf{x}$, \parallel and \perp refer to the directions in relation to the external magnetic field \mathbf{B} , respectively, $\rho_s \equiv \sqrt{\tau}\rho_i$, $\tau \equiv T_e/T_i$, λ_D is the electron Debye length and $\hat{\mathbf{b}} \equiv \mathbf{B}/B$ is the unit vector. This set of equations can be solved using the traditional PIC method by loading the distribution function, $F(\mathbf{x}, \mathbf{v}, t)$, inhomogeneously in the configuration space and following the particle trajectories by [7],

$$\frac{d\mathbf{x}}{dt} = v_{\parallel} \hat{\mathbf{b}} + \mathbf{v}_{E \times B} \quad (3)$$

and

$$\frac{dv_{\parallel}}{dt} = -\frac{q}{m} \frac{\partial \phi}{\partial x_{\parallel}}. \quad (4)$$

However, numerical noise could cause problems in the low density region in the simulation. One way to avoid the problem is by invoking the multiscale expansion of

$$\frac{\partial}{\partial \mathbf{x}} \rightarrow \frac{\partial}{\partial \epsilon \mathbf{x}} + \frac{\partial}{\partial \mathbf{x}},$$

where ϵ is a smallness parameter representing the variation of the background inhomogeneity, Eq. (1) then becomes

$$\frac{dF}{dt} = \mathbf{v}_{E \times B} \cdot \boldsymbol{\kappa} F, \quad (5)$$

and $\boldsymbol{\kappa} \equiv -(d \ln F / d \epsilon x) \hat{\mathbf{x}}$ represents the background inhomogeneity in density and temperature in the x direction. The advantage of this equation is that we can load the simulation particles homogeneously, since the background drive is separated out. This equation is the same as Eq. (24) in the paper by Lee in 1987 [8], where the author pointed out that this equation became an inhomogeneous equation in phase space and, as such, the standard particle simulation could not be used. Instead, an approximate method for particle pushing based on

$$\frac{d\mathbf{x}}{dt} = v_{\parallel} \hat{\mathbf{b}} + \mathbf{v}_{E \times B} - \frac{c}{B} \boldsymbol{\kappa} \times \hat{\mathbf{b}} \phi$$

along with Eq. (4) to solve for Eq. (5) was developed [8]. The method is not completely satisfactory because of the compressibility issue in phase space [1] (see also the Appendix of the present paper). But, that was before the concept of weighted particles had been introduced.

II. Particle-In-Cell (PIC) Simulation Schemes using Weighted Particles - Using weight-based simulation scheme to solve the full- F multiscale equation, Eq. (5), directly is certainly feasible, but we will postpone its discussion for a later paper. Instead, we will start from a simplified, but related, equation. For

$$F = F_0 + \delta f, \quad (6)$$

where either $\delta f \ll F_0$ or $\delta f \neq \delta f(\epsilon \mathbf{x})$, from Eq. (5), we get

$$\frac{dF}{dt} = \mathbf{v}_{E \times B} \cdot \boldsymbol{\kappa} F_0. \quad (7)$$

On the other hand, we can also use Eq. (1) of $dF/dt = 0$ to obtain the time evolution of the perturbed distribution as

$$\frac{d\delta f}{dt} = \mathbf{v}_{E \times B} \cdot \boldsymbol{\kappa} F_0 - \frac{q}{m} E_{\parallel} \frac{\partial F_0}{\partial v_{\parallel}}. \quad (8)$$

These two time evolution equations are similar but have different numerical properties. Based on the procedures first suggested by Dimits and Lee [1] and Parker and Lee [2], the perturbed distribution in Eq. (8) can be evaluated by

$$\delta f = wF, \quad (9)$$

where

$$\frac{dw}{dt} = (1 - w) \mathbf{v}_{E \times B} \cdot \boldsymbol{\kappa} - (1 - w) \frac{q}{m} E_{\parallel} \frac{1}{F_0} \frac{\partial F_0}{\partial v_{\parallel}}, \quad (10)$$

and the background inhomogeneity of

$$F(t = 0) = F_0(x) = n_0(x) \sqrt{\frac{m}{2\pi T_0(x)}} \exp\left[-\frac{mv_{\parallel}^2}{2T_0(x)}\right], \quad (11)$$

gives

$$\boldsymbol{\kappa} \equiv \kappa_n \hat{\mathbf{x}} - \left(1 - \frac{v_{\parallel}^2}{v_t^2}\right) \frac{\kappa_T}{2} \hat{\mathbf{x}}, \quad (12)$$

with $\kappa_n \equiv -d \ln n_0 / dx$ and $\kappa_T \equiv -d \ln T_0 / dx$, and $\partial F_0 / \partial v_{\parallel} = -(m/T_0) v_{\parallel} F_0$. As one can see, at $t = 0$, w is small, since the perturbed potential, ϕ , is small and, consequently, δf is small and quiet, while F is noisy as described by the Fluctuation-Dissipation Theorem (FDT) for a gyrokinetic plasma [8, 10].

We should remark here that F in Eq. (7) still contains the zeroth-order inhomogeneities as given by n_0 and T_0 in Eq. (11), so does δf via Eq. (9). Thus, we can still load particle inhomogeneously as prescribed by Eq. (11) in the simulation without double counting for the inhomogeneities in

Eq. (8). However, the noise property at the low density end of the simulation may become a problem, where less number of simulation particles would be used. To mitigate this problem, the zeroth-order homogeneous loading proposed by Parker and Lee [2] to minimize the noise problem has been widely used. Let us now re-visit this property by again introducing the new phase space distribution $G(\mathbf{x}, v_{\parallel}, t)$ which is homogeneous in the configuration space and Maxwellian in the velocity space, at $t = 0$, such that,

$$\frac{dG}{dt} = 0. \quad (13)$$

Now, let us define

$$p \equiv \frac{F}{G} \quad (14)$$

and

$$w \equiv \frac{\delta f}{G}, \quad (15)$$

where, as before, $F = F_0 + \delta f$ and F_0 is the zeroth-order distribution. Taking the convective derivative, d/dt , of Eqs. (14) and (15) and substituting with Eqs. (7), (8) and (13), we obtain

$$\frac{dp}{dt} = (p - w)\mathbf{v}_{E \times B} \cdot \boldsymbol{\kappa} \quad (16)$$

and

$$\frac{dw}{dt} = (p - w) \left(\mathbf{v}_{E \times B} \cdot \boldsymbol{\kappa} + \frac{q}{T} E_{\parallel} v_{\parallel} \right). \quad (17)$$

By setting $p = 1$ in Eq. (17), we recover Eq. (10) of the original one-weight scheme [2]. On the other hand, letting $(p - w) \rightarrow p'$ in Eqs. (16) and (17) to obtain dp'/dt , we then recover the two-weight scheme of Hu and Krommes [11]. Invoking the discrete Klimontovich-Dupree representation for the total distribution of a system with N particles at time t as

$$G(\mathbf{x}, v_{\parallel}, t) = \sum_{j=1}^N \delta[\mathbf{x} - \mathbf{x}_j(t)] \delta[v_{\parallel} - v_{\parallel j}(t)], \quad (18)$$

we can then represent the distribution functions of interest as

$$F(\mathbf{x}, v_{\parallel}, t) = \sum_{j=1}^N p_j(t) \delta[\mathbf{x} - \mathbf{x}_j(t)] \delta[v_{\parallel} - v_{\parallel j}(t)], \quad (19)$$

$$\delta f(\mathbf{x}, v_{\parallel}, t) = \sum_{j=1}^N w_j(t) \delta[\mathbf{x} - \mathbf{x}_j(t)] \delta[v_{\parallel} - v_{\parallel j}(t)], \quad (20)$$

where the time evolution of particles, $\mathbf{x}(t)$ and $v_{\parallel}(t)$, and their weights are given by Eq. (3), (4), (16) and (17), respectively. Together with Eq. (2), we have a complete system of equations. As

for the initial conditions, we can let $p = F_0(x)/\langle F_0(x) \rangle \approx 1$ and $w \ll 1$, where $\langle \dots \rangle$ is the spatial average.

Let us now describe the procedures for calculating the number density in gyrokinetic Poisson's equation, Eq. (2). From

$$n = n_0 + \delta n,$$

with

$$n(\mathbf{x}, t) = \int F dv_{\parallel} = \sum_{j=1}^N p_j(t) \delta[\mathbf{x} - \mathbf{x}_j(t)]$$

and

$$\delta n(\mathbf{x}, t) = \int \delta f dv_{\parallel} = \sum_{j=1}^N w_j(t) \delta[\mathbf{x} - \mathbf{x}_j(t)],$$

the gyrokinetic Poisson's equation can be evaluated numerically as

$$(\rho_s/\lambda_D)^2 \nabla_{\perp}^2 \phi = -4\pi e [c(n_i - n_e) + (1 - c)(\delta n_i - \delta n_e)]. \quad (21)$$

Since $p_j \sim o(1)$ and $w_j \sim o(\epsilon)$, where ϵ is a smallness parameter related to the perturbation, δn is much quieter numerically than n . It, therefore, makes sense to set $c = 0$ in the simulation at all times, which is essentially the reason behind the usual δf simulation [2]. On the other hand, in the fully nonlinear stage, it has been shown consistently that the fluctuation level of the ensuing turbulence is significantly above the thermal level in present-day tokamak transport simulations, see, for example, Ref. [12]. Therefore, it is feasible to make c in Eq. (21) time-dependent, for example, by setting $c(t = 0) = 0$, and changing, say, linearly and slowly to $c_1(t = t_1) = 1$ at a certain point in time in the simulation. The criterion is such that the signal of the resulting turbulence should always be much higher than the intrinsic noise due to discrete particle effects [8, 10]. As shown earlier [13], the intrinsic noise level, after initial transient, remains constant in time even in the present of microinstabilities. The proposed procedures are different from that of Qin et al. for simulating beam plasmas [14], for which the multiscale expansion was not used.

Let us now illustrate these procedures by simulating one-dimensional drift waves, which was studied earlier by Parker and Lee [2]. In this type of simulation, there is no spatial variation along the x (radial) direction. Thus, there is no actual diffusion along this direction, although the particle weights will evolve in time. As such, there is no nonlinear $\mathbf{E} \times \mathbf{B}$ trapping [15] nor the nonlinearly-generated zonal flows [4] in the simulation. The only nonlinear saturation mechanism is the nonlinear velocity space trapping [2], which is usually near the phase velocity of the wave

of interest with $\omega/k_{\parallel} \ll v_{te}$ and $\delta f/F \ll 1$. These are rather numerically-demanding simulations and many of the major simulation codes in the magnetic fusion community don't include this piece of important nonlinear physics. Using the same parameters as the earlier work [2], i.e., $k_y \rho_s = 0.75$, $\kappa_n \rho_s = 0.2$, $T_e/T_i = 1$, $m_i/m_e = 1837$, $\theta = 0.01$, $L_y/\rho_s = 8$, $N_{grid} = 16$, $N_{steps} = 4096$, and $\Omega_i \Delta t = 0.35$, where the external magnetic field is given by

$$\hat{\mathbf{b}} = \hat{\mathbf{b}}_z + \theta \hat{\mathbf{y}},$$

the density inhomogeneity κ_n is in the x direction [see Eq. (12)], v_{\parallel} is along the $\hat{\mathbf{b}}$ direction and the self-consistent fields associated Eqs. (1) and (2) are now given by $\mathbf{E} \times \hat{\mathbf{b}} = E_y \hat{\mathbf{x}}$, $E_{\parallel} = \theta E_y$ and $E_y = -\partial\phi/\partial y$, we have carried out the simulations of the most basic type of drift instabilities as follows.

First, the simulations via a one-dimensional code [16] written in MATLAB for $N_p = 1000$ particles running on an Intel MAC laptop are shown in Fig. 1, where the left panel (L) shows the results using the one-weight scheme of Parker and Lee [2] [i.e., Eq. (17) with $p = 1$] and the right panel (R) gives those using the two-weight scheme of Hu and Krommes [11] [i.e., Eqs. (16) and (17) with $(p - w) \rightarrow p'$]. For both cases, $c = 0$ is used for the gyrokinetic Poisson's equation, Eq. (21), at all times, with $w = 10^{-4}$ and $p = 1$ at $t = 0$ as the initial conditions. As expected, these two sets of results are very similar to each other. The linear frequency, the linear growth rate and the nonlinear saturation level of $\omega_L/\Omega_i \approx 0.1$, $\gamma_L/\Omega_i \approx 0.01$ and $|e\phi/T_e|_{NL} \approx 0.9\%$, respectively, are also very similar to those given in Ref. [2]. We should again emphasize here that the saturation of the drift waves in the simulation is due to the nonlinear wave-particle interaction through the *velocity space nonlinearity* term of $E_{\parallel}(\partial\delta f/\partial x_{\parallel})$ in Eq. (1). The average particle weight at the end of the simulation using the one-weight scheme [2] is about $\sqrt{\sum_{j=1}^{N_p} w_j^2/N_p} \approx 1.7\%$.

To test the δf to full- F transition, we have carried out the simulations by using Eqs. (16) and (17) with $c(t = 0) = 0$ in Eq. (21), which then evolve linearly to $c(t = t_1) = 1$ along with the initial conditions of $w = 10^{-4}$ and $p = 1$ at $t = 0$, and

$$t_1 = l N_{steps} \Delta t \quad (22)$$

in Eq. (21). By turning on the full- F simulation slowly, for example, the results for $l = 12$ with 10,000 particles are shown in the left panel of Fig. 2, where there is an 8.3% of full- F particle contribution at the end of the simulation. The results for $l = 10$ with 100,000 particles, where there is an 10% of full- F particle contribution at the end, are given at the right panel of

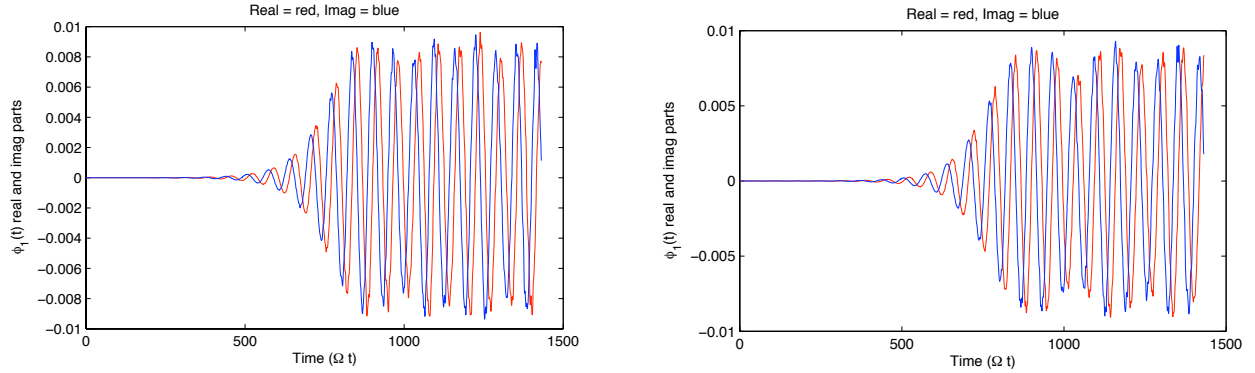


FIG. 1: One-weight δf (L) and two-weight δf (R) simulation results using $1K$ particles for $\Omega_i \Delta t = 0.35$

Fig. 2. As we can see, both of these results are very similar to those using the δf schemes in Fig. 1, in terms of the frequency, growth rate and saturation level. Thus, we can use more full- F particles when there are more particles in the simulation. However, when more full- F particles are used in the simulation, the saturation amplitude has been observed to grow larger in later times. On the other hand, by halving the time step of the simulation to $\Delta t = 0.175$, we are able to turn on the full- F response faster as shown in the left panel of Fig. 3 with $l = 5$ for 100,000 particles, where there are 20% of full- F particles at the end of the simulation. To verify the relationship between a larger number of simulation particles and a higher percentage of full- F particles, we have also used the code on the Linux cluster at PPPL. The results for the δf to full- F scheme with 1,000,000 particles using Eqs. (16) and (17), and Eq. (21) with

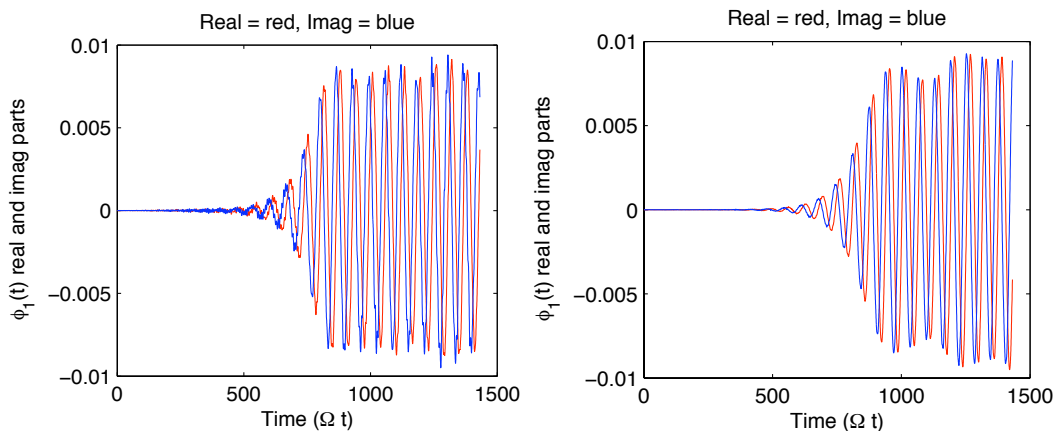


FIG. 2: Simulation for the δf + full- F scheme with (L) $l = 12$ using $10K$ particles and (R) $l = 10$ using $100K$ particles for $\Omega_i \Delta t = 0.35$, where l is defined in Eq. (22)

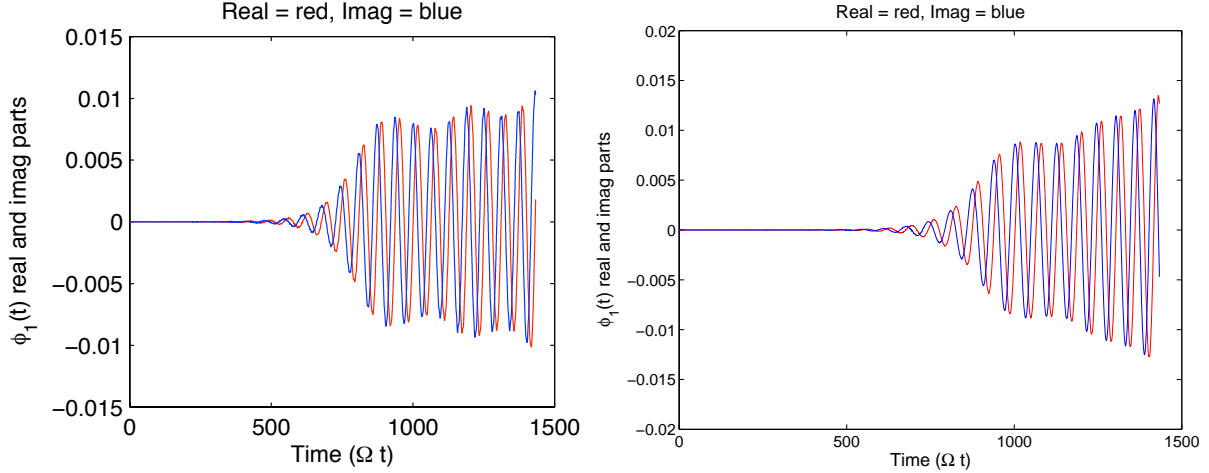


FIG. 3: Simulation results for the δf + full- F scheme with (L) $l = 5$ using $100K$ particles and (R) $l = 2$ using $1M$ particles for $\Omega_i \Delta t = 0.175$

$l = 2$ are given by the right panel of Fig. 3, where there are 50% full- F particles at the end of the run. The increase in the nonlinear fluctuation level due to numerical noise toward the end of the simulation is evident. The problem results from the feebleness of the nonlinear saturation from particle trapping, associated with the nonlinear $E_{\parallel} \partial \delta f / \partial v_{\parallel}$ term in Eq. (1) and can only be resolved by very high resolutions in the velocity space, compounded by the presence of the high frequency electrostatic shear-Alfven normal modes, $\omega_H [\equiv (k_{\parallel} / k_{\perp}) \sqrt{m_i / m_e} \Omega_i]$ [8, 17]. It is interesting to point out that this nonlinear trapping effect has been ignored in many of the fusion simulation codes, especially the Eulerian codes using the local approximation. This is partly due to the fact that, in realistic tokamak simulations [3–6], the nonlinear effects due to $\mathbf{E} \times \mathbf{B}$ trapping and the nonlinearly generated zonal flows ($m = 0, n = 0$), accompanied by energy cascade to the longer wavelength modes [3–6], are believed to be much more dominant in the nonlinear stage of the simulation. However, in the collisionless steady state, the velocity space nonlinearity is the essential ingredient for entropy balance [18]. Thus, it should not be ignored in the simulation.

But, we can do anything about the ω_H modes and the associated noise in the nonlinear stage. As we know, there are two ways to deal with the ω_H noise in the simulation. One is the δf scheme [2] and the other is the split-weight scheme [19]. Both are perturbative schemes and the latter eliminates the ω_H modes from the simulation entirely. The proposed δf to full F scheme takes advantage of the unique feature that the problem of particle noise is most severe at the beginning of the simulation, and is mitigated considerably in the nonlinear stage when the fluctuation

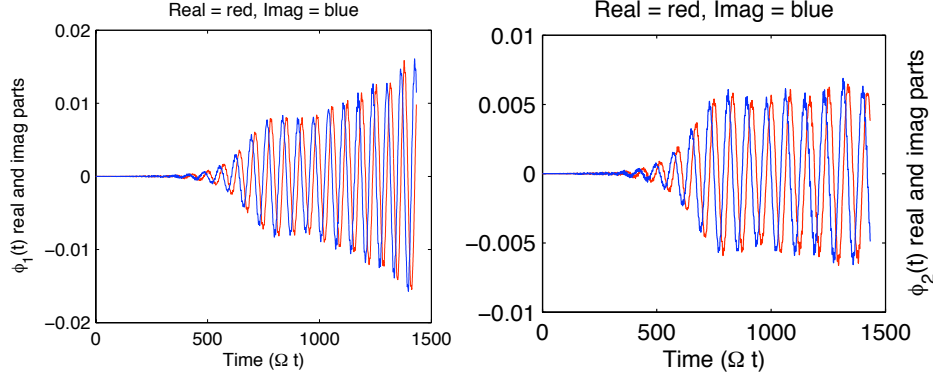


FIG. 4: δf to full- F simulations for $l = 1$ with 100K particles with the parameter (L) $\alpha = 1$ and (R) $\alpha = 2$ in the modified gyrokinetic Poisson's equation, Eq. (23), for $\Omega_i \Delta t = 0.175$

amplitudes of the instability are much higher than those generated by the intrinsic noise. The validity of the present scheme also related to the findings by Jenkins and Lee [13] which show that the saturation amplitude is independent of the intrinsic particle noise and the level for the intrinsic noise, given by the fluctuation-dissipation theorem for an equilibrium plasmas, does not grow with the instability. However, the noise problem still persists in the nonlinear stage as shown here unless we use even more particles and/or smaller time steps.

One possibility to mitigate this noise problem is to borrow the idea from the split-weight scheme [19] through the modification of the gyrokinetic Poisson's equation, Eq. (21), by subtract the adiabatic response on both sides of the equation so as to minimize the impact of ω_H modes, i.e.,

$$(\rho_s^2 \nabla^2 - \alpha c) \frac{e\phi}{T_e} = -\frac{c(n_i - n_e) + (1 - c)(\delta n_i - \delta n_e)}{n_0} - \alpha c \frac{e\phi}{T_e}, \quad (23)$$

where α is a constant. Simulations have been carried out for the δf to full- F scheme with 100,000 particles using Eqs. (16) and (17), starting with $c(t = 0) = 0$ and changing linearly to $c(t = t_1) = 1$ in Eq. (23), where t_1 is specified by Eq. (22). For the usual initial conditions for p and w at $t = 0$, $\alpha = 1$ and $l = 1$, i.e., there are 100% full- F particles at the end of the simulation, the results are shown in the left panel of Fig. 4. As one can see, the frequency and the saturation amplitude are correct, but the fluctuation starts to grow again shortly after the saturation. For the case of $\alpha = 2$, as shown in the right panel of Fig. 4, the oscillation amplitude remains constant after saturation. Although the overall magnitude is slightly lower in comparison with those in Fig. 1, we nevertheless believe that these are very encouraging results. For both of these simulations, only one iteration was used at each time step in solving Eq. (23), starting first with $\phi = 0$ on the

right hand side.

Finally, for comparison purposes, we have also carried out full- F simulations with 100,000 and 1,000,000 particles using Eqs. (16) and (17) with $c = 1$ in Eq. (21) and $p = 1$ at $t = 0$. As expected, in agreement with previous findings [16], the instabilities never saturated although the frequency seemed more reasonable with more particles. The time evolutions resembled those at the end of the simulations given by Figs. 3(R) and 4(L).

IV. Conclusions

In the present paper, a generalized two-weight scheme for collisionless plasma is proposed, which can be used to simulate microturbulence in tokamaks by first use the δf scheme to minimize the numerical noise before gradually switching to the full- F scheme. The work was inspired by several previous attempts on the subject and, particularly, by the thesis work of Jenkins [16]. The proposed procedures, either using Eq. (21) or Eq. (23), should result in considerable savings in computing resources, especially the latter. Moreover, the latter is readily applicable to simulate ITG modes in tokamak plasmas, where adiabatic electron response is routinely assumed, by solving the gyrokinetic Poisson equation of the form,

$$(\rho_s^2 \nabla^2 - 1) \frac{e\phi}{T_e} = - \frac{cn_i + (1-c)\delta n_i}{n_0}, \quad (24)$$

and by starting with $c = 0$ and ending with $c = 1$. Simulations of ITG modes with large weight are nothing new. For example, the average particle weight of $\sqrt{\sum w^2 / N_p} \approx 28\%$ has been observed at the end of the δf simulation of turbulence transport on tokamak plasmas [12]. Applying this generalized weight-based PIC scheme to tokamak plasmas with sources and sinks will be a logical next step. On the other hand, a more self-consistent full- F scheme to account for the adiabatic response similar to the split-weight scheme [19] may be needed. Collisional effects associated with these schemes are another important research area. The two-weight scheme by Wang et al. [20] could serve that purpose. We should also mention that weight-based numerical schemes to solve the multiscale equation of the form of Eq. (5) directly with homogeneous loading is presently under investigation and the results will be published elsewhere, which would give us another viable alternative to carry out full- F simulations. In the future, the full- F simulation may be important for the integrated modeling of microturbulence and MHD physics based on the global PIC simulation of tokamak plasmas and there is no doubt that other similar PIC schemes will be developed for that purpose. However, no matter what PIC methods one chooses, they should

preserve the property of incompressibility of the phase space fluid for the full- F distribution as given in the appendix.

Appendix - Particle-In-Cell Simulation of Incompressible Phase Space Fluid

Let us first start with the Vlasov equation for a collisionless unmagnetized plasmas, which can be written as

$$\frac{dF}{dt} \equiv \frac{\partial F}{\partial t} + v \frac{\partial F}{\partial x} + \frac{q}{m} E \frac{\partial F}{\partial v} = 0, \quad (25)$$

where $F(x, v, t)$ is the distribution function, which, in the Klimontovich-Dupree representation, can be expressed as

$$F(x, v, t) = \sum_{j=1}^N \delta[x - x_j(t)] \delta[v - v_j(t)], \quad (26)$$

where N is the number of particles in the system. Taking the time derivative of the distribution function, we have

$$\frac{\partial F}{\partial t} = \sum_{j=1}^N \left[\frac{dx_j}{dt} \frac{\partial}{\partial x_j} + \frac{dv_j}{dt} \frac{\partial}{\partial v_j} \right] \delta[x - x_j(t)] \delta[v - v_j(t)],$$

which gives

$$\frac{\partial F}{\partial t} = \sum_{j=1}^N \left[v_j \frac{\partial}{\partial x_j} + \frac{q}{m} E_j \frac{\partial}{\partial v_j} \right] \delta[x - x_j(t)] \delta[v - v_j(t)],$$

since the equations of motion of the particles are

$$\frac{dx_j}{dt} = v_j, \quad (27)$$

$$\frac{dv_j}{dt} = v \frac{q}{m} E_j \quad (28)$$

and $E_j \equiv E(x_j)$. In turn, we obtain,

$$\frac{\partial F}{\partial t} = \sum_{j=1}^N \left[\frac{\partial}{\partial x_j} v_j + \frac{q}{m} \frac{\partial}{\partial v_j} E_j \right] \delta[x - x_j(t)] \delta[v - v_j(t)],$$

since neither v_j is a function of x_j nor E_j is a function of v_j . From the relationship of

$$f(x) \delta(x - a) = f(a) \delta(x - a),$$

the time derivative of F takes the form of

$$\frac{\partial F}{\partial t} = \sum_{j=1}^N \left[\frac{\partial}{\partial x_j} v + \frac{q}{m} \frac{\partial}{\partial v_j} E(x) \right] \delta[x - x_j(t)] \delta[v - v_j(t)].$$

From the Dirac form of the delta function,

$$\delta(x) = \lim_{\epsilon \rightarrow 0} \frac{1}{\pi} \frac{\epsilon}{x^2 + \epsilon^2},$$

it can be shown easily that

$$\frac{d\delta(x-a)}{dx} = -\frac{d\delta(x-a)}{da}.$$

We then obtain

$$\frac{\partial F}{\partial t} = -\sum_{j=1}^N \left[\frac{\partial}{\partial x} v + \frac{q}{m} \frac{\partial}{\partial v} E(x) \right] \delta[x - x_j(t)] \delta[v - v_j(t)].$$

Substituting the definition of F given by Eq. (26) into the above expression, we obtain

$$\frac{\partial F}{\partial t} + \frac{\partial}{\partial x}(vF) + \frac{q}{m} \frac{\partial}{\partial v}(EF) = 0,$$

which is the equation we solve when pushing particles. For a Hamiltonian system, we recover Eq. (25). Thus, Eq. (25) describes an incompressible fluid in phase - the *Vlasov Fluid*. This property of incompressibility should be satisfied in the simulation at all times.

-
- [1] A. M. Dimits and W. W. Lee, J. Comp. Phys. **107**, 309 (1993).
 - [2] S. E. Parker and W. W. Lee, Phys. Fluids B **5**, 77 (1993).
 - [3] S. E. Parker, W. W. Lee and R. A. Santoro, Phys. Rev. Lett. **71**, 2042 (1993).
 - [4] Z. Lin, T. S. Hahm, W. W. Lee, W. M. Tang, and R. White, Science **281**, 1835 (1998).
 - [5] W. X. Wang, T. S. Hahm, S. Ethier, G. Rewoldt, W. W. Lee, W. M. Tang, S. M. Kaye, and P. H. Diamond, Phys. Rev. Lett. **102**, 035005 (2009).
 - [6] Y. Xiao and Z. Lin, Phys. Rev. Lett. **103**, 085004 (2009).
 - [7] W. W. Lee, Phys. Fluids **26**, 556 (1983).
 - [8] W. W. Lee, J. Comput. Phys. **72**, 243 (1987).
 - [9] W. W. Lee and H. Qin, Phys. Plasmas **10**, 3196 (2003).
 - [10] J. A. Krommes, W. W. Lee and C. Oberman, Phys. Fluids **29**, 2421 (1986).
 - [11] G. Hu and J. A. Krommes, Phys. Plasmas **1**, 863 (1994).
 - [12] W. W. Lee, S. Ethier, R. Kolesnikov, W. X. Wang, and W. M. Tang, Computational Science & Discovery **1**, 015010 (2008).
 - [13] T. G. Jenkins and W. W. Lee, Phys. Plasmas **14**, 032307 (2007).

- [14] H. Qin, R. C. Davidson and E. A. Startsev, *Phys. Plasmas* **15**, 063101 (2008).
- [15] W. W. Lee, J. A. Krommes, C. R. Oberman, and R. A. Smith, *Phys. Fluids* **27**, 2652 (1984).
- [16] T. G. Jenkins, Ph. D. Thesis, Princeton University (2007).
- [17] W. W. Lee, J. L. V. Lewandowski, T. S. Hahm and Z. Lin, *Phys. Plasmas* **8**, 4435 (2001).
- [18] W. W. Lee and W. M. Tang, *Phys. Fluids* **31**, 612 (1988).
- [19] I. Manuilskiy and W. W. Lee, *Phys. Plasmas*, **7**, 1381 (2000).
- [20] W. X. Wang, N. Nakajima, M. Okamoto, and S. Murakami, *Plasma Phys. Controlled Fusion* **41**, 1091 (1999).

The Princeton Plasma Physics Laboratory is operated
by Princeton University under contract
with the U.S. Department of Energy.

Information Services
Princeton Plasma Physics Laboratory
P.O. Box 451
Princeton, NJ 08543

Phone: 609-243-2245
Fax: 609-243-2751
e-mail: pppl_info@pppl.gov
Internet Address: <http://www.pppl.gov>